Relationships between greenhouse gas production and landscape position during short-term permafrost thaw under anaerobic conditions in the Lena Delta

Mélissa Laurent[1], Matthias Fuchs[1], Tanja Herbst[1], Alexandra Runge[1], Susanne Liebner[2,3], Claire C. Treat[1]

[1]Alfred Wegener Institute Helmholtz Centre for Polar and Marine Research, Potsdam, Germany
[2] GFZ German Research Centre for Geosciences, Section Geomicrobiology, Potsdam, Germany
[3] University of Potsdam, Institute for Biochemistry and Biology, Potsdam, Germany

Correspondence to: Mélissa Laurent (melissa.laurent@awi.de)

Abstract. Soils in the permafrost region have acted as carbon sinks for thousands of years. As a result of global warming, permafrost soils are thawing and will potentially release greenhouse gases (GHGs) such as methane (CH_4) and carbon dioxide (CO_2). However, small scale spatial heterogeneities of GHG production have been neglected in previous incubation studies. Here, we used an anaerobic incubation experiment to simulate permafrost thaw along a transect from upland Yedoma to floodplain in Kurungnakh Island. Potential CO_2 and CH_4 production were measured during incubation of active layer and permafrost soils at 4 °C and 20°C, first for 60 days (approximate length of growing season), and then continuing for one year. An assessment of methanogen abundance was performed in parallel for the first 60 days. Yedoma samples from upland and slope cores remained in a lag phase during the growing season simulation, while those located in the floodplain showed high production of CH_4 (6.5×10^3 µg CH_4-C g^{-1} C) and CO_2 (6.9×10^3 µg CO_2-C g^{-1} C) at 20°C. The Yedoma samples from the permafrost layer started producing CH_4 after six months of incubation. We conclude that landscape position is a key factor triggering CH_4 production during the growing season time in Kurungnakh Island.

Summary. Climate change is causing increasing temperatures and permafrost thaw, which might lead to increases in the release of the greenhouse gases CO_2 and CH_4. In this study, we investigated the effect of different parameters (temperature, landscape position) on the production of these gases during a one-year permafrost thaw experiment. For very similar carbon and nitrogen contents, our results show a strong heterogeneity in CH_4 production, as well as in microbial abundance. According to our study, these differences are mainly due to the landscape position and the hydrological conditions established as a result of the topography.

1 Introduction

For the past decades, scientists have warned about the effects of global climate change (IPCC 2021). The effects of this warming will be pronounced in the polar regions where the air temperature increase in the past fifty years is already three times higher than the increase in global average during the same period (AMAP, 2021; Rantanen et al., 2022). This particularly affects soils in northern high latitude permafrost regions, which cover 14.6% of the Northern Hemisphere (Obu et al., 2019) and contain 1300 Pg of organic carbon (C) (Hugelius et al., 2014a). A majority of this C (822 Pg) is stored in permafrost (Hugelius et al., 2014b), which is defined as ground where the temperature remains at or below 0 °C for more than two consecutive years (Washburn, 1973). Due to low temperatures, the organic matter (OM) stored in permafrost soils is characterized by low decomposition rate (Davidson and Janssens, 2006). However, during summer, the upper part of the permafrost affected soils thaws (active layer) and allows OM decomposition (Lee et al., 2012). With climate change, permafrost thaw will likely increase and lead to higher OM decomposition rates, releasing greenhouse gases (GHGs), like carbon dioxide (CO_2), and methane (CH_4) (Wagner et al., 2007; Schuur et al., 2015; Knoblauch et al., 2018).This turnover

might lead to the transformation of Arctic soils from C sinks to C sources (Koven et al., 2011; Dean et al., 2018; Lara et al., 2019).

Carbon emissions, and mainly CH_4 emissions greatly vary across Arctic, and especially within small scales (Treat et al., 2018; Lara et al., 2019; Elder et al., 2020). Treat et al. (2018) showed that C flux variability was strongly associated with specific landscape types due to differences in soil moisture and site drainage in uplands and wetlands that also controlled vegetation communities, which we are referring to here as landscape position. Landscape change due to permafrost thaw is also highly affected by landscape position: low-lying ice-rich areas can become waterlogged following permafrost thaw, while higher areas can be drained by water run-off (Osterkamp et al., 2009; Liljedahl et al., 2016). The water-logged areas like thermokarst lakes or wetlands have been identified as CH_4 emissions hotspots (Olefeldt et al., 2013; Treat et al., 2018b; Kuhn et al., 2021) because of the anaerobic conditions that favour methanogen communities (Conrad, 2002; Yavitt et al., 2006). On the other hand, well-drained sites, such as upland tundra, have the capacity to offset CH_4 emissions by acting as CH_4 sinks due to net oxidation in the surface soil layer (Juncher Jørgensen et al., 2015; Treat et al., 2018). Hence, after permafrost thaw, the redox conditions, determined by the landscape position, lead to different microbial communities and ultimately different CH_4 emissions (McCalley et al., 2014).

To quantify CH_4 and CO_2 production and to understand C turnover from thawing permafrost, numerous incubation studies have been carried out (Lee et al., 2012; Knoblauch et al., 2018; Walz et al., 2018; Holm et al., 2020). Studies have shown that C decomposition depends on several factors, such as organic C quantity, OM quality, temperature, and oxygen availability in the soil (Ganzert et al., 2007; Lee et al., 2012; Schädel et al., 2014; Treat et al., 2015; Knoblauch et al., 2018). In addition, Treat et al. (2015) highlighted that CH_4 production differences were partly explained by the landscape position, with differences between uplands, wetlands, floodplain soils, lowlands, and drained lake basins. For incubation under aerobic conditions, Kuhry et al. (2020) demonstrated that landscape types based on soil type (peaty wetlands, mineral soils) and the origin of the deposits (peat deposits, alluvial deposits) gave a good estimation of SOM lability, and therefore explained differences in CO_2 production better than using only the %C, which is a commonly used metric for C quality across incubation studies (Treat et al., 2015). However, few studies have specifically focused on how the landscape position affects CO_2 and CH_4 production under anaerobic conditions, and whether landscape position is a good indicator of CO_2 and CH_4 production under anaerobic conditions as might be expected from field observations of CO_2 and CH_4 fluxes (Treat et al., 2018; Elder et al., 2020).

Besides landscape position, climate change affects the environmental factors in the study region. It modifies weather conditions and plays a key role in controlling rain events (frequency and intensity) (Callaghan et al., 2010; Tabari, 2020; Wang et al., 2021; Fewster et al., 2022). During the past 60 years, precipitation in Siberia has increased by 2.6 mm/decade over the year Wang et al., (2021). This finding leads likely to wetter conditions during the growing season in Siberia, and therefore, soil moisture increases. Changes in soil moisture will impact vegetation cover and soil redox conditions. Increasing precipitation and warming will also lead to deepening of the active layer (Zhu et al., 2017; Douglas et al., 2020), hence, release bioavailable C from the upper part of the permafrost layers. Waldrop et al. (2010) identified more labile C in shallow permafrost than in the active layer, which fuelled more CO_2 production in an incubation experiment. On the other hand, other incubation experiments showed higher C turnover and more CO_2 production in the active layer than in the permafrost (Walz et al., 2017; Faucherre et al., 2018). Regarding CH_4 production, incubation studies tend to show higher CH_4 production in the active layer than in shallow permafrost (Treat et al., 2015), but some studies also measured the opposite behaviour among their samples (Wagner et al., 2007; Waldrop et al., 2010). Therefore, it is still unclear how much CO_2 and CH_4 can be produced from shallow permafrost. Furthermore, high CH_4 production heterogeneity as well as long lag time have been measured with samples from Kurungnakh Island, Lena Delta, Russia (Knoblauch et al., 2013, 2018). Hence, the question remains whether the methanogen communities will have the time to become active during the short growing season (60 days) under anaerobic condition.

The aim of this study was to simulate permafrost thaw under wet growing season conditions across different landscape units in the Lena Delta, and measure CO_2 and CH_4 production. Here, we incubated upland Yedoma and adjacent lowland floodplain samples under anaerobic conditions, and focused on the relationships between GHG production and microbial abundance shifts following short-term (60 days, growing season length) and longer-term (1 year) permafrost thaw. The objectives of the study were to: (1) quantify CH_4 and CO_2 production over one year under anaerobic incubation; (2) establish relationships between CH_4 and CO_2 production and methanogen abundances; and (3) characterize the role of the landscape position on gas production in thawed permafrost soils during a growing-season time frame.

2 Materials and methods

2.1 Site description and sampling

Soil samples were collected in August 2018 on Kurungnakh Island (72.333° N, 126.283° E), Lena Delta, Siberia (Figure 1). Kurungnakh Island is located in the continuous permafrost zone and is an erosional remnant of Late Pleistocene deposits, characterized by ice- and organic-rich sediments (Grigoriev, 1993; Schwamborn et al., 2002); most of the island is composed of fluvial sandy sediments and Yedoma Ice Complex (IC) deposits. The IC is made up of ice-saturated sediments (65% to 90%), composed of cryoturbated silty sands and peaty deposits of Holocene origin (Schwamborn et al., 2002; Schirrmeister et al., 2011, 2013). Sediments from the Yedoma IC contain on average 3% total organic carbon (TOC) (Strauss et al., 2013a), however, IC sediments can include organic-rich layers, with TOC content reaching more than 20% in layers contained within the ice complex sediments (e.g. buried peat horizons, Andreev et al., 2009). Kurungnakh Island is characterised by thermokarst lakes and wetlands due to thermo-erosional activity (Morgenstern et al., 2021). Samples were also collected in the young Kurungnakh Island floodplain area. The young and active floodplains in the Lena River Delta are of Holocene deltaic origin and are composed of stratified middle to fine sands and silts with layers of autochthonous peat and allochtonous OM (Schwamborn et al., 2002; Boike et al., 2013).

The soil sampling was carried out in two stages. First, the active layer was extracted using a spade, and active layer samples were collected using a fixed volume cylinder (250 cm^3). Then, permafrost soil cores were sampled to a depth of one meter below surface, by drilling with a modified snow ice and permafrost (SPIRE) auger (Jon Holmgren's Machine Shop, Alaska, USA). For this study, three cores were selected, two were from the Yedoma deposits (P15 and P16) and one belonged to a floodplain area (P17). The three coring locations were on a well-drained upland soil (P15; Supplementary Fig 1), on a north-eastern facing slope (P16), and on a floodplain (P17; Figure 1). The floodplain samples were taken in the highest part of the floodplain, 5 m above the Lena River water level.

These cores were chosen on the basis of geographical proximity to each other, landscape position, moisture gradient, and ice composition. The three cores had an organic layer ranging between 3 to 7 cm (Yedoma and floodplain, respectively). Below this organic surface layer, the soil cores were identified as mineral soil. The permafrost layers from the Yedoma cores were ice-rich, while no visible ice structure was seen for the floodplain core (Table 1).

Cores were described and subsampled in the field. Detailed core descriptions are presented in Table 1 and Supplementary Table 1. For the purpose of our study, we chose two samples from each core, one from the active layer and one from the frozen layer (above 1 m depth to simulate shallow permafrost thaw; Supplementary Table 1). Care was taken not to select samples from the top of the active layer in order to avoid the top organic layers. Cores were subsampled in a climate chamber at -4 °C with a hammer and a chisel instead of a saw, to limit contamination.
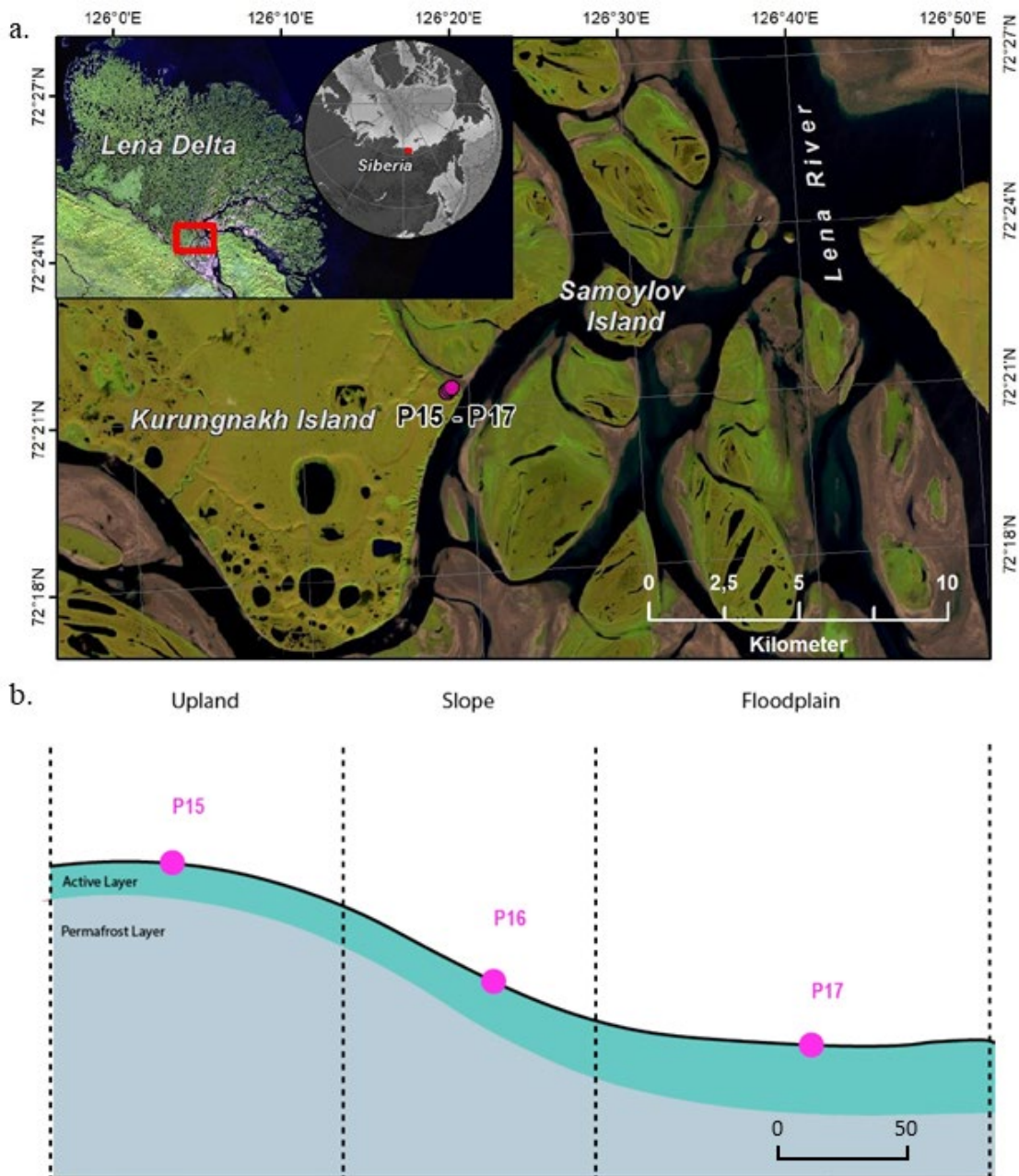
120

Figure 1: Location of Kurungnakh Island in the Lena Delta (Siberia). The location of the cores used for the study are indicated on the map (a.) and along a schematic transect (b.). Samples were taken during the Lena summer expedition in 2018.

2.2 Sedimentary and geochemical characterization

125   We characterized the samples for soil texture, C and nitrogen contents, water content, conductivity, and pH. First, samples were thawed at 4° C overnight; then the pore water was extracted with a rhizon soil moisture sampler (Rhizon MOM - 0.6 μm Rhizosphere) (Meijboom and van Noordwijk, 1991). Electrical conductivity and pH were measured from pore water. Prior to further analyses, soil samples were freeze-dried, and the absolute water content (Eq 1) was calculated. For TOC weight percent, Total Carbon (TC), and Total Nitrogen (TN), subsamples were homogenized and measured with a carbon-nitrogen-sulfur

130   (CNS) analyzer (Elementar Vario EL III). Each subsample was measured in duplicate, and standards and blanks were used to ensure reliable analytical measurements. The bulk density was determined based on a transfer function between absolute water content and bulk density made by Fuchs (2019) (Supplementary Fig 2). Since most of the samples used to establish this correlation came from the same area as our samples, we assumed that the transfer function was applicable to our samples.

$$\theta = \frac{W_w - W_d}{W_w} \quad \text{Eq(1)}$$

135 Where θ is the water content, W_w is wet weight, and W_d dry weight.

Carbon storage was calculated by multiplying the TOC contents with the bulk density and then divided by the sample length. Another subsample was used for grain size characterization. The grain size analysis was conducted using a laser diffraction particle size analyzer (Mastersizer 3000, Company Malvern, Malvern, UK). Prior to measuring, subsamples were put on a

140 heated shaker for three weeks, and H_2O_2 was added daily to remove the organic materials. The samples were measured in a wet dispersion unit, and at least three subsamples from each sample were measured. The average grain size distribution (in vol%) was calculated from the measured replicates.

2.3 Incubation set-up and substrate addition

145 To mimic a wet growing season, the samples were first incubated under anaerobic conditions for 60 days at two different temperatures, 4 °C and 20 °C. Since eleven samples out of twelve did not produce CH_4 after two months incubation, we extended the incubation time to 363 days to see whether the other cores would produce CH_4. For every sample, three replicates were incubated, resulting in a total of 36 samples. Prior to incubation, the samples were thawed at 4°C and prepared under oxygen-free conditions using an anoxic glovebox. The samples were homogenized and 13 g of wet soil was collected and

150 inserted into a 120 mL vial. Sterilized tap water was added only to samples with a gravimetric moisture content of less than 30% to limit the effect of gas dissolution (Henry's Law). The amount of sterilized tap water was calculated to reach 30% gravimetric moisture, based on the original water content and the weight (wet and dry). The flasks were closed with rubber stoppers and aluminium lids. The headspace of the samples was flushed with pure nitrogen for three minutes to remove potential O_2 inside the vials. Then the samples were incubated in the dark.

155 After 60 days of incubation, 0.7 mg glucose per gram dry sample weight were added to two of the three replicates to understand the effect of potential substrate limitation in the soil system. The glucose was diluted with milli-Q water to obtain a 100 g.L^{-1} solution. Solutions were injected via syringe to minimize soil disturbance (Pegoraro et al., 2019). The same amount of water as in the glucose solution was added to the third replicate to ensure that differences in gas production were only due to the addition of glucose (Pegoraro et al., 2019; Adamczyk et al., 2021). The glucose addition was also carried out under oxygen-

160 free conditions.

The effects of glucose are usually observed within less than 48 h (Yavitt et al., 1997; Pegoraro et al., 2019). Therefore, after the glucose addition, gas was measured daily for one week (described in the following section). As the first injection had little effect on gas production, a second injection (day 64) was added with twice the amount of glucose solution (1.4 mg glucose per gram dry sample weight).

165 2.4 Gas analyses

CO_2 and CH_4 in the headspace were measured with a gas chromatograph (GC) (7890A, Agilent Technologies, USA) with flame ionization detection (FID). The temperature in the column was 50 °C with a flow of 15 mL min^{-1} and a runtime of 4.5 minutes. Helium was used as a carrier gas. A Hamilton syringe was used to introduce 250 µL of the sampling gas into the GC. For the first week, measurements were made every two days, then twice a week for three weeks, then once a week until day

170 60. The incubation vials were flushed when either CH_4 or CO_2 concentration reached 10^4 ppm to avoid gas saturation inside the flask. The production rate was calculated with the change in concentration of CO_2 and CH_4 over the incubation time. First the measured CO_2 and CH_4 concentrations were converted from ppmv to µmol L^{-1} using the ideal gas law, then a linear regression between each measurement point was used to calculate the change in concentration over time. The production rate was calculated using the change in concentration over time from the linear regression, then the rates were normalized using

175   the volume of the soil (for differences in the jar headspace) and the weight of the dry soil samples (Robertson et al., 1999). Then these rates were also normalized by the %C found in each sample to look at substrate quality. For samples with pH>7, water contents were very low (Table 1), therefore we assumed that a negligible amount of CO_2 was stored as DIC in the sample water and did not correct the calculation for the pH. However, we are aware that this might underestimate C mineralization.

180   The impact of glucose on CH_4 and CO_2 production was quantified as a glucose factor, calculated using the cumulative C production at 67 days.

$$Gf = \frac{(P_{gt} - P_t)}{P_t}$$

Where Gf is the glucose factor, P_{gt} is total CH_4 production for samples with glucose, and P_t is total CH_4 production.

2.5 Quantification of methanotrophic and methanogenic gene copy numbers

185   Methanogenic archaea were quantified with quantitative Polymerase Chain Reaction (qPCR) at different times during the incubations: when the samples were still frozen (1); after 60 days of incubation (2); and after glucose addition (67 days of incubation) (3). However, due to laboratory restrictions during the Covid-19 pandemic, it was not possible to analyse all the incubated vials. Only one replicate per sample for the first two runs were analysed. For the last run, we selected the two samples with the highest CH_4 production rates after the glucose addition – the active layers of P16 and P17.

190   Since methanotrophic bacteria are good indicators of the oxidation level under in-situ conditions, they were quantified with qPCR before starting the incubation.

Key genes encoding the enzyme methyl coenzyme-M reductase (*mcrA*) (Thauer, 1998) and for the enzyme particulate methane monooxygenase (*pmoA*) (Theisen and Murrell, 2005) were examined to identify methanogens and methanotrophs, respectively. DNA extractions were performed with a GeneMATRIX Soil DNA purification kit (Roboklon, Germany)

195   according to the manufacturer's protocol. After DNA extraction, the DNA concentration was quantified by fluorescence with the Qubit dsDNA HS Assay Kit (Invitrogen, United States). Gene copy numbers were quantified using a SYBRGreen qPCR assay using the KAPA SYBRFAST qPCR Master Mix (Sigma-Aldrich, Germany) on a CFX96 real-time thermal cycler (Bio-Rad Laboratories Inc., United States). All runs were performed in technical triplicates, and each run was completed through melt-curve analysis in order to check for specificity of the assay (Liebner et al., 2015). Methanogenic archaea were targeted

200   with the primer set mlas-F/*mcrA*-R (Microysynth, Balgach, Switzerland) (Hales et al., 1996).

To amplify the methanogenic archaea *mcrA* gene, PCR samples were kept at 95 °C for 5 min to denature the DNA. The amplification process was performed with 40 denaturation cycles at 95°C for 1 min, annealing at 60 °C for 45 s, and elongating at 72 °C for 90 s. To ensure complete amplification, samples were kept at 80 °C for 10 min. In addition, to amplify the methanotrophic *pmoA* gene, using primer pmoA189-F and primer pmoAmb661-R two PCR reaction conditions were used.

205   The first PCR comprised initial denaturation at 95 °C for 5 min, 30 cycles with denaturation at 94 °C for 45 s, decreasing annealing temperature from 64 °C to 52 °C for 60 s, elongation at 72 °C for 90s, and final elongation at 80 °C for 90 s. The second PCR comprised an initial denaturation and polymerase activation at 95 °C for 5 min, 22 cycles of denaturation at 94 °C for 45 s, annealing at 56°C for 60 s, elongation at 72 °C for 90 s, and a final extension at 72 °C for 10 min.

2.6 Statistical analyses

210   The gas production and microbial data did not show a normal distribution; consequently, it was not possible to test for differences by performing an ANOVA. The differences between cores and depths, and also the impact of temperature on gas production and microbes, were therefore tested using the Kruskal-Wallis test with the R function, kruskal.test().

All statistics and results analyses were performed with R version 4.0.5 (R Core Team, 2021).

3 Results

3.1 Soil characteristics

All soil samples had a pH between 6.5 -7.5, except P15-F. Most electrical conductivities were very low (<200 µS.cm^{-1}), except for two samples: P16-F and P17-A (Table 2). Water content was higher in permafrost (54.5%-60.8%) than in the active layer (23.7%-25.8%) for the two yedoma cores, P15 and P16. The water content was higher in the active layer than the permafrost layer in the floodplain core P17 (36.2% vs. 17.2%; Table 2).

Sediment TOC ranged from 0.2% to 3.8%. Most TOC contents ranged from 2.7% to 3.8% but the TOC content in the permafrost layer of P17 was the lowest of the six samples (0.17%; Table 2). All the samples had TOC below 6%, and therefore they were considered as mineral soils (%C < 12%) (Table 2) (Soil Survey Staff, 2014). TN contents were very low for all the samples (<0.3%) and was below the detection limit of the laser analyzer (below 0.1%) for P17-F. C:N ratios ranged between 12 and 20. The highest ratios were measured in P15; the lowest were in P16. The C:N ratio was higher in the permafrost layer of P15 than in the active layer.

The C stock ranged from 2.3 to 38.8 kg.m^{-3}. The active layers for all the samples were higher than 30 kg.m^{-2} while, the highest C stock in the permafrost layer was 19 kg.m^{-3} in the Yedoma core P16. The permafrost layer of the floodplain had the lowest C storage, more than ten times lower than samples from the active layers (Table 2).

The grain size distribution was similar between P15 and P16. The active layer of P17 contained more clay and the least sand of the other samples, while permafrost in P17-F was the sandiest sample (Supplementary Table 1).

Table 1: Soil description and vertical position of the sampling cores.

Samples	Depth (cm)	Layer	Horizon	Soil description
P15-A	41.5	Active	Mineral	Compacts silt, grey, with brown organic inclusions
P15-F	81.5	Permafrost	Mineral	Ataxilic ice structure, silt grey
P16-A	38.5	Active	Mineral	Silt, brown, organic rich, slightly sandy
P16-F	102.5	Permafrost	Mineral	Silt, grey-brown, structureless to micro-lenticular
P17-A	31.5	Active	Mineral	Organic rich silt, slighlty sandy
P17-F	78.5	Permafrost	Mineral	Sand, no visible ice

Table 2: Chemical and physical properties of the active and frozen layers of the three cores. The conductivity temperature reference was 25°C. Numbers in brackets are standard deviations

Samples	pH	Conductivity (µS/cm)	TOC (%)	C/N ratio	TN (%)	C (kg.m^{-3})	Water content (weight %)
P15-A	6.75	164.5	3.54	18.13	0.1975	38.8	25.8
P15-F	6.06	150.2	2.70	20.59	0.133	9.4	60.8
P16-A	7.21	98.6	2.70	12.95	0.211	35.2	23.7
P16-F	7.06	479	3.81	12.67	0.3085	18.5	54.5
P17-A	7.22	635	3.48	18.46	0.1935	30.0	36.2
P17-F	7.44	86.4	0.17		< 0.10	2.3	17.2

3.2 Potential gas production

3.2.1 CH$_4$ production over one year of incubation

At the end of 363-day incubation, four of the six samples produced CH$_4$ at 20 °C incubation temperature (Figure 2; Figure 3). The floodplain active layer (P17-A) was the sample with the highest cumulative CH$_4$ production over the incubation time (917.2 ± 150 µg CH$_4$-C g^{-1} DW). After 6 months of incubation, the CH$_4$ production rate of P17-A decreased and then plateaued. The floodplain permafrost core (P17-F) produced 1% of the amount of CH$_4$ produced by the active layer from the same core (0.5 ± 0.2 µg CH$_4$-C g^{-1} DW) at 20 °C. The permafrost layers at 20 °C of both Yedoma cores (P15 and P16) produced similar amounts of CH$_4$ (20.5 ± 6.1 µg CH$_4$-C g^{-1} DW and 159 ± 104 µg CH$_4$-C g^{-1} DW, respectively) while CH$_4$ production from the active layers of these cores was minimal (P16-A: 3.34 ± 0.25 µg CH$_4$-C g^{-1} DW; P15-A: 0.51± 0.14 µg CH$_4$-C g^{-1} DW). Cumulative CH$_4$ production at 4°C was limited to one sample, the active layer of the floodplain core (Figure 2; Figure 3). Cumulative production of the other cores was less than 1 µg CH$_4$-C g DW^{-1} after 1 year (Figure 2a; Figure 2b; Figure 3).

The lag time before CH$_4$ production was observed ranged from 14 days to over 363 days. The active layer of the floodplain core (P17-A-20) was the first to produce CH$_4$ after 14 days of incubation at 20 °C. The frozen layers of Yedoma the cores required at least 6 months incubation to start producing CH$_4$ at 20 °C (Figure 2; Table 2), but in the active layer of the Yedoma cores, CH$_4$ production took substantially longer: 273 days for P16-A-20, while P15-A did not produce appreciable CH$_4$ over 363 days in the experiment. At 4 °C, CH$_4$ production in P17-A started after 333 days but was not observed for the other samples (Figure 2; Table 3).

3.2.2 CO$_2$ production over one year of incubation

Over the 363-day incubation, cumulative CO$_2$ production ranged from 90.3 to 701.4 µg CO$_2$-C g^{-1} DW. The cumulative CO$_2$ production of P17-A at 20 °C was the highest among all the samples (701.4 ± 124 µg CO$_2$-C g^{-1} DW), while the permafrost layer of the same core at 20 °C was the lowest (Figure 2; Figure 3). The CO$_2$ production of P15 and P16 were in the same range, between 142 ± 85 µg CO$_2$-C g^{-1} DW (P16-A at 4 °C) and 348.3 ± 135 µg CO$_2$-C g^{-1} DW (P15-F at 20 °C) (except P16-F at 4 °C); (Chi squared = 2.80, df = 1, p = 0.20) (Figure 2; Figure 3). At 4°C, the permafrost layers of the Yedoma core P16 and the floodplain core P17 had cumulative production below 60 µg CO$_2$-C g^{-1} DW. The results per g C showed a different pattern for the cumulative CO$_2$ production of the floodplain core P17. The permafrost layer at 4 °C reached 7.98 mg CO$_2$-C g^{-1} C and had higher CO$_2$ production than the permafrost layer at 20 °C and the active layer at 4 °C. (Supplementary Fig 3)

A decrease of CO$_2$ production at the beginning of the incubation was observed for all the samples (Figure 2, Supplementary Fig 4). All the active layer samples (except the active layer of the floodplain P17 at 4 °C), as well as the permafrost layers of the Yedoma cores P15 and P16 at 20 °C, reached the maximum production rates of CO$_2$ before or at the end of the first two months (Figure 2). The maximum production rate of CO$_2$ for the active layer of the floodplain at 4°C was attained after 300-day incubation, and the other permafrost samples reached the maximum production rate between two and five months (Figure 2). Maximum production rates ranged between 57.13 µg C-CO$_2$ g C^{-1} d^{-1} (P16-A) and 754 µg C-CO$_2$ g C^{-1} d^{-1} (P17-F) at 4 °C, and between 120.54 and 510.65 µg C-CO$_2$ g C^{-1} d^{-1} for P16-F and P15-A, respectively, at 20 °C (Supplementary Table 2). After half a year of incubation, CO$_2$ production plateaued for all the samples, except for the active layer of the floodplain sample at 4 °C. For all the samples, we noticed an increase in CO$_2$ production after 60 days of incubation, e.g., after the microbial sampling, followed by a decrease in the CO$_2$ production. We did not consider those results to describe the maximum production rates.

After one year of incubation, neither the temperature nor the depth impacted the cumulative CO$_2$ production of the cores (Chi squared = 3.86, df = 1, p = 0.09), Figure 2, Figure 3). CO$_2$ production was higher at 20 °C only for the permafrost layer of the Yedoma core P16 and the active layer of the floodplain P17 (Chi squared = 3.86, df = 1, p < 0.05) (Figure 2; Figure 3).

The P17-A-20 CO_2:CH_4 ratio decreased rapidly during the first 14 days. The CO_2:CH_4 ratio reached one after 40 days and remained stable until the end of incubation (Table 2). As well, the CO_2:CH_4 ratio of P17-A at 4°C and P16-F at 20 °C were low after 363 days of incubation (respectively, 2.7 ± 2.7 and 2.5 ± 2.1). For all the samples, except P15-F, CO_2:CH_4 ratios were significantly lower at 20 °C than at 4 °C (Chi squared = 3.92, df = 1, p < 0.05) (Table 3).

280
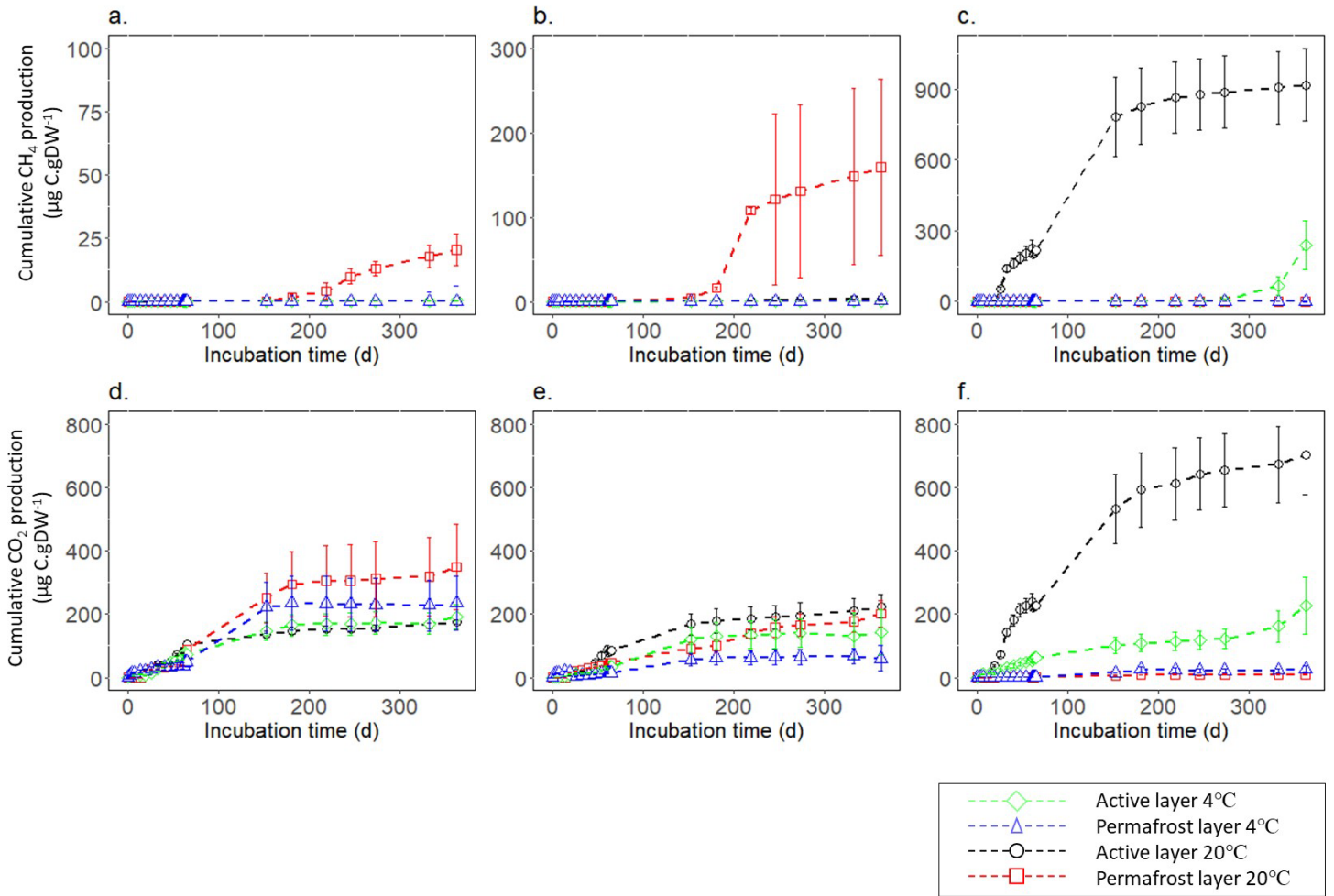
Figure 2: Cumulative gas production per gram dry weight (DW) at 4 °C and 20 °C for 363 days of incubation. CH_4 production of (a.) P15, (b.) P16 and (c.) P17. CO_2 production of (d.) P15, (e.) P16 and (f.) P17. Error bars show the standard deviation from the means ± standard error (n=3). Note differing y-axis scales between cores for CH_4

285

Figure 3: Cumulative production of CO₂ and CH₄ per gram dry wet after 60 days of incubation at 4°C and 20°C and after 363 days. AL stands for "Active layer" and PL stands for "Permafrost Layer". Scale is expressed as square root for a better representation of the data.
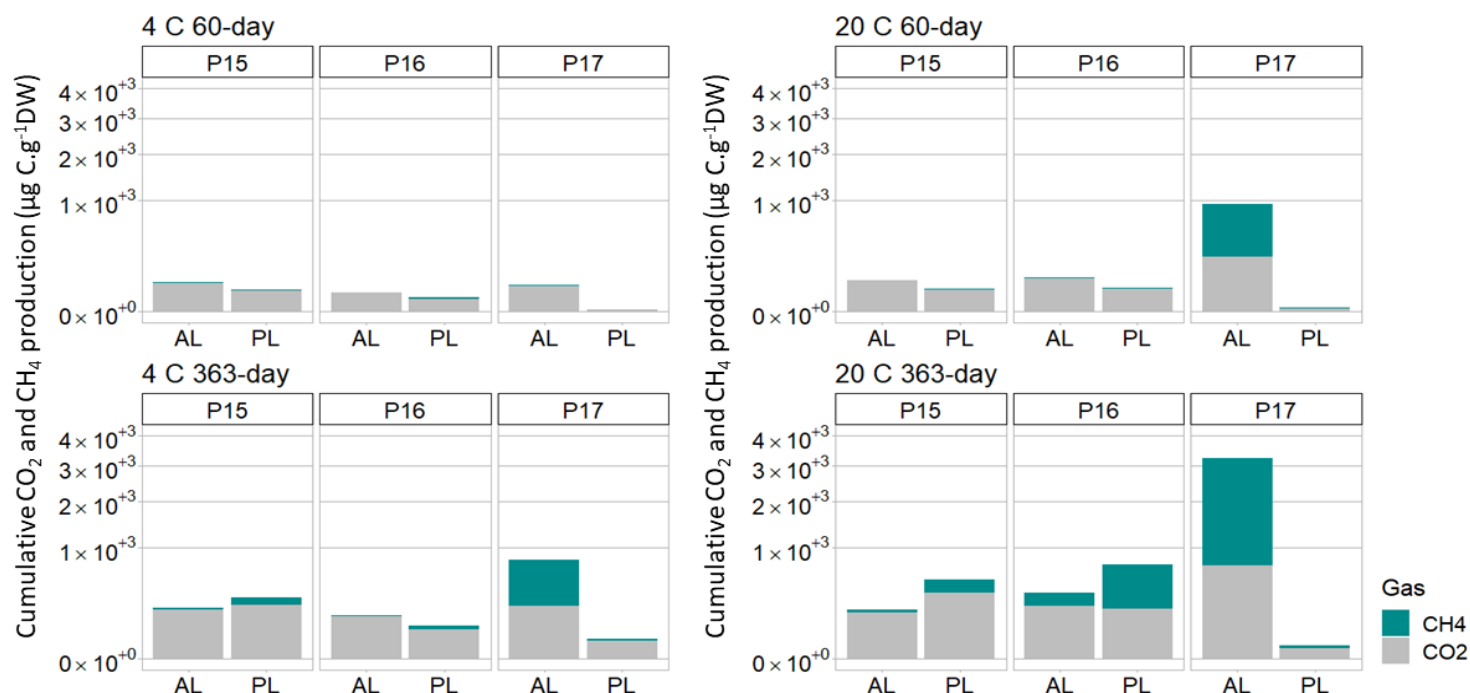
290

Table 3: Summary of lag time of CH₄ offset, CO₂:CH₄ ratios, and glucose factors. Lag time is expressed in days, L.T. stands for samples where the lag time did not end after 1 year incubation. CO₂:CH₄ ratios represent means of total production after 363 days of incubation at 20 °C and 4 °C after 363 days of incubation. Glucose factors were calculated based on cumulative C production 7 days after glucose addition. Positive values indicate positive impact of glucose on GHG production while negative values indicate less GHG production after glucose addition.

295

Samples	Layer	Lag Time (days)		Mean CO₂:CH₄		Glucose Factor			
		20 °C	4 °C	4 °C	20 °C	CH₄ 4 °C	CH₄ 20 °C	CO₂ 4 °C	CO₂ 20 °C
P15-A	Active	L.T.	L.T.	$522.6 \pm 1.7 \times 10^{+2}$	$409.1 \pm 2.2 \times 10^{+2}$	-0.10	-0.38	0.02	0.18
P15-F	Permafrost	153	L.T.	$1930.1 \pm 2.2 \times 10^{+3}$	$2236.8 \pm 3.9 \times 10^{+3}$	0.02	-0.31	-0.20	-0.44
P16-A	Active	274	L.T.	$1661.4 \pm 1.5 \times 10^{+2}$	$50.1 \pm 4.0 \times 10^{+1}$	-0.41	0.70	-0.02	1.22
P16-F	Permafrost	181	L.T.	$195.5 \pm 1.3 \times 10^{+2}$	2.5 ± 2.1	0.40	-0.93	0.11	3.23
P17-A	Active	14	333	2.7 ± 2.7	0.8 ± 0.1	-0.01	0.24	0.51	0.60
P17-F	Permafrost	L.T.	L.T.	$266.9 \pm 1.8 \times 10^{+2}$	$34.8 \pm 4.2 \times 10^{+1}$	1.18	0.27	-0.11	0.82

3.2.3 Effect of glucose addition

Overall, no effect of glucose injection on CH_4 production was detected after 67-day incubation (Table 3) (Chi squared = 0.25, df = 1, p = 0.5913). A CH_4 production peak was detected one day after the second glucose addition for P15 and P16. The response factors were low (CH_4 production between 1.2 and 1.7 times higher with glucose addition than without) and appeared only at 20 °C. No impact of the glucose addition was detected on CH_4 production for the samples at 4 °C, neither after the first nor the second injection (Supplementary Figure 5).

CO_2 production at 20 °C was in overall increased by glucose (Chi squared = 3.78, df = 1, p < 0.05). The maximum increase of CO_2 production was seen for the permafrost layer of P16 (4.2 times higher with glucose addition). No difference in CO_2 production was detected for any of the samples at 4 °C after glucose addition (Supplementary Figure 5).

3.3 Gene copy numbers of methanogens and methanotrophs

For half of the samples, no methanogenic gene copy numbers were detected when the samples were thawed prior to beginning the incubation. From these samples, only the methanogenic gene copy number for core P17-A was above the detection limit (4.3×10^3). Therefore, it was not possible to compare the methanogenic gene copy numbers before the start of the incubation (Figure 4).

After 60 days of incubation, the *mcrA* gene copy numbers ranged from 5.35×10^3 to 5.34×10^5. The qPCR results showed significant differences between cores after 60 days of incubation (Chi squared = 3.89, df = 1, p < 0.05) with the highest copy number per gram soil (Figure 4c) in P17-A. No methanogenic gene copy numbers were detected for the permafrost layer of P17, as well as the active layer of P16.

P16-F and P17-A had 9 and 36 times higher mcrA copy number per gram soil, respectively, at 20 °C than at 4 °C (Chi squared = 3.9, df = 1, p < 0.05) (Figure 4). The temperature response for the active and permafrost layer of P15 was not identified because the results were below the detection limit both at 4 °C and 20 °C.

Similarly, no comparison was possible between active and permafrost layers for all the samples.

Gene copy numbers of methanotrophic bacteria based on the *pmoA* gene, were either below detection limit or not detected before the incubation, therefore no interpretation on the oxic conditions under field condition was possible (Figure 4).

Copy numbers after addition of glucose did not differ from those without glucose (Figure 4).
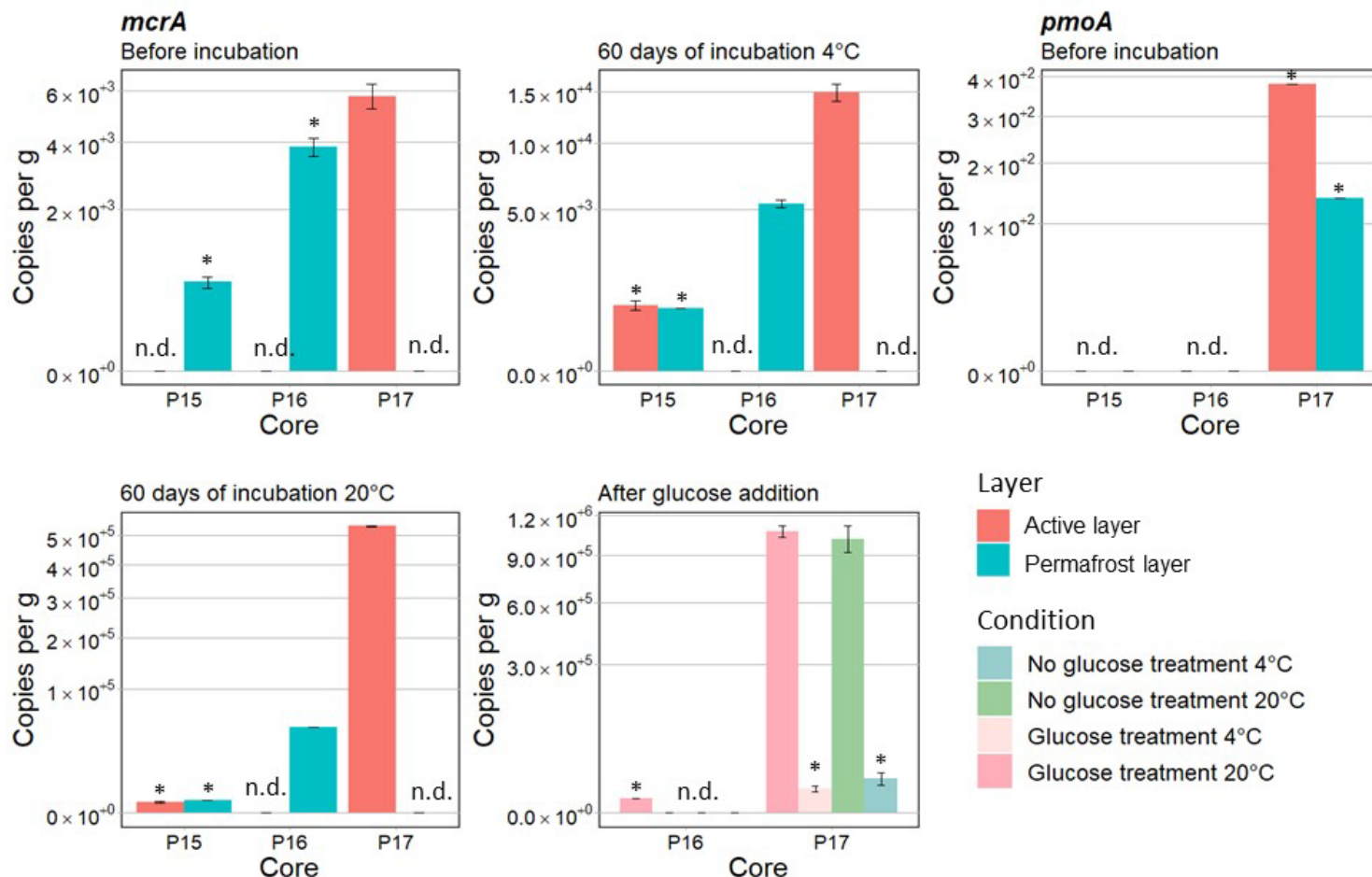
Figure 4: Means of gene copies per gram calculated with qPCR amplification at different time for different conditions - before the incubation, after 60 days of incubation, and at the end. Gene copy numbers of *mcrA* were calculated for P15, P16, and P17. *mcrA* results are shown for the active layers of P16 and P17 with or without glucose treatment after 67 days of incubation. Gene copy numbers of *pmoA* are shown for P15, P16, and P17 before the incubation. Samples below detection limit are indicated by * and samples where copies per gram were not detected are indicated by n.d. Scale is expressed as square root in order to have a better display.

4. Discussion

4.1. CH_4 production in floodplain environment and Yedoma cores across landscape positions

4.1.1. Floodplain core

We mimicked potential CH_4 production during a growing season (60 days) in a floodplain environment of Kurungnakh Island in the Lena River Delta, and extended the incubation time to one year to capture the CH_4 production behavior. Within the first two months, the results showed high rates and quick onset of CH_4 production as well as presence of methanogen communities (Figure 4) in the active layer of the floodplain core P17 at 20 °C only. Those findings, as well as the low $CO_2:CH_4$ ratio, indicated a quick establishment of optimum methanogenic conditions within the growing season time frame of 60 days (Symons and Buswell, 1993) (Figure 2c, Figure 3, Table 3). Herbst (2022) did a similar incubation study with samples from the active floodplains of Kurungnakh Island and nearby Samoylov Island (Figure 1). CH_4 was produced from two of the three cores within the first 60 days of incubation (Supplementary Table 3). In both this study and the Herbst study, CH_4 production was triggered quickly after the beginning of incubation (from 10 to 40 days) from these floodplain samples. Thus, these Arctic floodplain environments may allow the fast establishment of methanogens, and therefore, rapid CH_4 production under anaerobic conditions.

However, not all floodplain soils showed fast establishment of methane communities and high rates of potential methane production. Unlike the active layer, the permafrost layers of floodplain did not produce appreciable CH_4 after one year incubation at either 4°C or 20 °C and were still considered in the lag phase. The absence of detectable *mcrA* copy numbers per gram soil after 60 days of incubation indicated the absence of methanogen communities in the permafrost samples (Figure 4). Similarly, low rates of CO_2 production, low C content, and high sand content in this permafrost sample indicate non suitable conditions for many types of soil microbes (Figure 2, Figure 4, Table 1) (Eskelinen et al., 2009).

As expected, our results showed significant differences between CH_4 production rates at 4 °C and 20 °C. At 4 °C, almost 300 days of incubation were needed to trigger CH_4 production in the active layer of the floodplain (versus 14 days at 20°C), with a total cumulative CH_4 production four times lower than at 20 °C (Figure 3). Other studies showed similar patterns, e.g., CH_4 production increases with temperature and has shorter lag times (Ganzert et al., 2007; Treat et al., 2015). This is explained by a strong temperature sensitivity of methanogen communities (Westermann, 1993; Li et al., 2015). At the end of the growing season simulation, our results showed *mcrA* copy numbers 36 times lower at 4 °C than at 20 °C (Figure 4), again indicating that the methanogen community required both time and high temperatures to establish.

4.1.2. Yedoma cores

This study highlights a different CH_4 production behavior between the floodplain and the Yedoma cores. The permafrost layers from the Yedoma cores only started producing CH_4 after six months of incubation at 20 °C, whereas the floodplain core produced CH_4 earlier (Figure 2). The CO_2:CH_4 ratios remained high after one year of incubation (Table 3), meaning that the methanogenic conditions were not yet optimum (Symons and Buswell, 1993). The low mcrA copies after the 60 days of incubation compared to the active layer of the floodplain, as well as the long lag times, showed that the methanogen communities took more time to become active in the permafrost Yedoma cores (Figure 2, Figure 4).

Our results indicated higher CH_4 production rates in the permafrost layer than in the active layer, while others generally show the opposite (Yavitt et al., 2006; Treat et al., 2015, p.201). However, most of the studies on CH_4 production from Yedoma cores showed high variability in the cumulative CH_4 production. As explained above, lag times measured from former studies differed as well as CH_4 production rates (Lee et al., 2012; Knoblauch et al., 2013; Walz et al., 2018; Jongejans et al., 2021). It is therefore difficult to estimate the potential production of CH_4 after thaw from Yedoma soils after thawing due to this high variability. Methanogens are highly constrained microbial communities, and the community size varied strongly between the sites in this study (Figure 4), which partly explains the discrepancies among the studies on Yedoma soils due to the ecological and phylogenetic narrowness of the methanogen communities (Ernakovich et al., 2022).

The active layers at 4 °C and 20 °C and permafrost layers at 4 °C were still in the lag phase without appreciable CH_4 production after one year of incubation (Figure 2, Figure 3, Table 3), which agrees with the absence of detected methanogen community (Figure 4). Several multiannual studies observed also long and heterogeneous lag times at 4°C for Yedoma soils (from 53±23 to up to 2500 days; Knoblauch et al., 2018; Walz et al., 2018). Knoblauch et al. (2018) explained the long lag time by a lack of methanogens, or a lack of active methanogenic communities in soil samples. We added glucose to test whether the absence of CH_4 production was due to a lack of labile C or to a lack of established methanogenic communities. If the methanogen community was small, but established, we would expect to have community growth after the glucose addition. Since glucose had no effect neither on CH_4 production rates nor on P15 and P16 methanogen community growth, we concluded that the absence of CH_4 production for those samples was because the methanogens were not active (or not active enough to detect). It has been shown that the establishment of microbial community after thaw is correlated to the community characteristics as well as the thaw disturbance (Deng et al., 2015; Ernakovich et al., 2022). For ecologically and phylogenetically narrow microbial communities, like methanogens, random environmental processes like microtopography (stochastic processes) strongly influence the abundances and activation of the microbial communities. After an abrupt thaw, like we simulated in our incubation study, the role played by stochastic processes on constrained microbial communities is even stronger (Deng et al.,

2015; Ernakovich et al., 2022). Therefore, although the incubation was carried out under anaerobic conditions, the quantity and the establishment of active methanogen community in the samples after thaw was strongly controlled by stochastic processes.

4.1.3. Controls on CH₄ production across landscape positions

CH_4 production over the incubation time was not correlated with the TOC and TN% (Figure 3, Table 2). The landscape position rather than soil characteristics played a key role in the establishment of microbial activity and, consequently, explained much of the variation in GHG production among the samples. Periodic water saturation in core P17 was indicated by oxidation marks at several depths in the field. These redox features indicate periodically anoxic conditions that likely favoured the establishment or persistence of methanogen communities and reduced the lag times prior to CH_4 production under anaerobic conditions (Chasar et al., 2000; Paul et al., 2006; Jaatinen et al., 2007; Keller and Bridgham, 2007; Figure 2, Table 3). On the other hand, well-drained conditions were found in the field for the active layers of both the upland and the slope cores (P15 and P16), which did not produce appreciable CH_4 after one year of incubation (Figure 2, Figure 3). The aerobic conditions due to the dry environment likely inhibited methanogenesis (Megonigal and Schlesinger, 2002). Unlike the active layers, the permafrost layers of Yedoma showed low but existing *mcrA* results from the Yedoma permafrost layers at 20 °C (Figure 4), and started producing CH_4 after six months. The methanogen community was likely established prior to or during the deposit of the Yedoma sediments and the microbial community survived although it was freeze-locked (Holm et al 2020). In addition, we quantified methanotroph communities to include more information about the potential for methane oxidation under field conditions, but the results showed amounts below detection limit before the incubation (Figure 4). These results support our hypothesis concerning the impact of landscape position on CH_4 production: aerobic conditions in the landscape coincided with poor establishment of methanogenesis even when incubation conditions become favourable for methanogens.

4.2. Controls on potential CO₂ production

The rates of CO_2 production per g C were in the same order of magnitude as other Yedoma incubation studies from Kurungnakh Island (Knoblauch et al., 2013, 2018) and nearby Lena River Delta (Walz et al., 2018). These similar results suggest that C in these Yedoma soils is easily available due to the organic-rich characteristics (Strauss et al., 2013). On the other hand, the adjacent samples from the permafrost layers of the floodplain showed CO_2 production g per gram similar to the Yedoma cores, while it had the lowest CO_2 cumulative production per gram dry weight of soil. Although floodplain environments in the Lena Delta are considered as a low C content pool (Siewert et al., 2016), our results showed that the C in this soil was highly labile and comparable to the lability of Yedoma soils.

The CO_2 production followed trends in total C and N contents. The samples with similar C and N contents produced comparable ranges of CO_2, whereas the sample (P17-F) with the lowest TOC and N content showed low CO_2 production (per gram DW) during the incubation (Figure 2, Table 2, Supplementary Table 2). As shown by Schaedel et al. (2014), the C:N ratio was positively correlated to the cumulative CO_2 production. However, the correlation was stronger at 4°C than 20 °C (Supplementary Fig 7). Therefore, consistent with other studies (Schädel et al., 2014; Knoblauch et al., 2018), the quality (N), quantity (C), and the bioavailability (C:N) of the OM is a key factor for the mineralization into CO_2 production.

Our CO_2 and CH_4 production results combined with microbial analysis indicated that CO_2 production pathways might change according to the landscape position. The CO_2:CH_4 production ratio of 1:1, as well as the presence of a high number of methanogenic archaea, indicated that the CO_2 production in the active layer floodplain could have originated from methanogenesis (Figure 3, Figure 4) (Symons and Buswell, 1993; Knoblauch et al., 2018; Holm et al., 2020). In drier environments, like the P15 and P16 cores, the high CO_2:CH_4 production rates resulted from other, undetermined anaerobic decomposition pathways. Anaerobic respiration is a common function, and diverse microbial communities are able to

decompose the OM to CO_2, therefore, the anaerobic microbial community is not a limiting factor for C mineralization to CO_2 (Elderfield and Schlesinger, 1998). Based on the positive correlation between C:N and the cumulative CO_2 (Supplementary Fig 7), and the broad microbial community able to produce CO_2, our CO_2 production is rather controlled by the quality (N) and the quantity (TOC) of the OM than the microbial communities (Knoblauch et al., 2018; Holm et al., 2020).

435

4.3. Implication for C feedback in Kurungnakh Island during the growing season

With climate change, Arctic environments will be subject to changes in moisture conditions, vegetation shifts, increased active layer depth and abrupt permafrost thaw (Serreze et al., 2000; Hinzman et al., 2005; Myers-Smith et al., 2011; Turetsky et al., 2019). Our permafrost thaw simulation under wet summer conditions for Kurungnakh Island soil showed that the CO_2

440   production for the Yedoma cores was similar in magnitude to other studies including Yedoma soil. In the incubation experiment, all the Yedoma samples reached the maximum production rates within the first two months of incubation (Figure 2). Schädel et al. (2014) attributed the decrease in CO_2 production rates after some time in incubations to a rapid C turnover that relied mainly on the decomposition of the labile C pool (Schädel et al., 2014; Walz et al., 2018; Schädel et al., 2020). However, several studies pointed out the small size of the labile C pool of Yedoma deposits (Knoblauch et al., 2013; Strauss

445   et al., 2013b). Here, the Yedoma soils from Kurungnakh Island showed labile C pool depletion after six months of incubation (e.g., the CO_2 production rates decreased and the cumulative CO_2 production plateaued after six months of incubation; Figure 2). Therefore, under wet summer conditions, it is likely that there will be rapid C turnover and CO_2 production during the growing season.

The active layer of the floodplain at 20 °C produced up to 300 µg CH_4-C g^{-1} DW at the end of the simulated growing season.

450   The low-lying position of the floodplain allows regular flooding from the river. The hydrological conditions of this area provide favorable redox conditions, i.e., anaerobic conditions, for the establishment of active methanogen communities if the temperature is high enough (Figures 3, 4). Therefore, we expect CH_4 production from the floodplain site relatively quickly after the beginning of the growing season. Long-term *in situ* measurements in the Lena Delta have shown the highest CH_4 emission rates for moist to dry dwarf shrub-dominated tundra, located mainly in lower floodplain environments (5048.5 mg

455   m^{-2} yr^{-1}; Schneider et al., 2009). In this area of the Lena Delta, CH_4 emissions have been measured from June to September, with the highest emission rates in July (Rößger et al., 2022). Our results showed a high CH_4 production potential from the floodplain, however, floodplain environments are periodically flooded, meaning there might be periods were the floodplain would be too dry to allow CH_4 production (Huissteden et al., 2005; Oblogov et al., 2020). A long-term study like by Rößger et al. (2022) in floodplains environments would help to quantify CH_4 emissions from floodplains, how often it occurs during

460   the growing season, and how the CH_4 flux would respond to changes in soil moisture over time.

While CH_4 production did occur in the year-long anaerobic incubation of Yedoma samples, other factors might result in these tundra regions still remaining a net CH_4 sink barring abrupt permafrost thaw (Schneider et al., 2009; Juncher Jørgensen et al., 2015). In these dry Yedoma sites, the net CH_4 flux is the balance between CH_4 production in anoxic soil layers and CH_4 oxidation in overlying aerobic layers. Here, we showed that CH_4 production was possible from these soils given high enough

465   temperatures (Figure 3), but required a long lag time for the establishment of the methanogen communities (Figure 4). Therefore, it is unlikely that the active methanogen communities have enough time (>60 days; Figure 4) or warm enough temperatures (Figure 3) to establish during the growing season in the upland and the slope areas (P15, P16) on Kurungnakh Island even with deeper active layers, soil moisture increases, and highly bioavailable C in Yedoma sediments (Anthony et al., 2014; Mann et al., 2014; Spencer et al., 2015). These conditions may constrain the potential CH_4 emissions from some Yedoma

470   soils even with warmer climates, wetter soils, and permafrost thaw, but will require additional field-based observations to account for plant transport and methane oxidation processes occurring in-situ.

5 Conclusion

In this study we provide new information regarding the importance of the landscape position for CH_4 production during the growing season in Kurungnakh Island in the Lena River Delta. High CH_4 production was measured in waterlogged (floodplain) areas within the 60 days simulation of the growing season at 20 °C, thanks to a fast establishment of the methanogen community (14 days). In contrast, the well-drained Yedoma active layer samples were still in the lag phase at the end of the growing season simulation and did not produce appreciable CH_4 emissions, and C turnover resulted in CO_2 production. CH_4 was produced by the Yedoma permafrost layers after a lag phase of six months at 20 °C. Although the permafrost layer of the floodplain had low TOC, we identified similar C lability for the three cores as for other studies with samples from Siberia, and therefore high potential C gas production throughout this region, but mainly as CO_2. As a result, the data presented in this case study contribute to quantifying and understanding C turnover in permafrost areas. Questions remain regarding how to upscale results from laboratory incubation to in-situ conditions, and our results highlighted the need to better understand changes in redox conditions across the landscape position to improve upscaling.

Author contributions

M.L., C.T. and S.L. designed the study. M.L. conducted all the experiments (soil analyses, incubations, and microbe quantification). M.F. and A.R. collected the soil samples and field notes during the expedition in 2018 and created the map. S.L. furnished laboratory materials to perform microbe analyses and gas measurements. T.H. provided data from her incubation experiments. M.L wrote the manuscript with contributions from all the co-authors.

Acknowledgments

Funding for this study was provided by ERC-H2020 #851181 FluxWIN, the Helmholtz Impulse Initiative and Networking Fund. Samples were collected during the joint Russian-German LENA 2018 expedition to Samoylov Island within the framework of the BMBF KoPf (Kohlenstoff in Permafrost) project (#3F0764B). This project was also supported by the European Erasmus+ programme. We thank the staff at the Samoylov Research Station for support and logistics during the fieldwork. We also thank the Alfred-Wegener Institute and GFZ lab technicians in Potsdam for laboratory assistance.

References

Adamczyk, M., Rüthi, J., and Frey, B.: Root exudates increase soil respiration and alter microbial community structure in alpine permafrost and active layer soils, Environmental Microbiology, 23, 2152–2168, https://doi.org/10.1111/1462-2920.15383, 2021.

AMAP: Arctic Climate Change Update 2021: Key Trends and Impacts. Summary for Policy-makers, 2021.

Andreev, A. A., Grosse, G., Schirrmeister, L., Kuznetsova, T. V., Kuzmina, S. A., Bobrov, A. A., Tarasov, P. E., Novenko, E. Y., Meyer, H., Derevyagin, A. Y., Kienast, F., Bryantseva, A., and Kunitsky, V. V.: Weichselian and Holocene palaeoenvironmental history of the Bol'shoy Lyakhovsky Island, New Siberian Archipelago, Arctic Siberia, Boreas, 38, 72–110, https://doi.org/10.1111/j.1502-3885.2008.00039.x, 2009.

Anthony, K. M. W., Zimov, S. A., Grosse, G., Jones, M. C., Anthony, P. M., Iii, F. S. C., Finlay, J. C., Mack, M. C., Davydov, S., Frenzel, P., and Frolking, S.: A shift of thermokarst lakes from carbon sources to sinks during the Holocene epoch, Nature, 511, 452–456, https://doi.org/10.1038/nature13560, 2014.

Boike, J., Kattenstroth, B., Abramova, K., Bornemann, N., Chetverova, A., Fedorova, I., Fröb, K., Grigoriev, M., Grüber, M., Kutzbach, L., Langer, M., Minke, M., Muster, S., Piel, K., Pfeiffer, E.-M., Stoof, G., Westermann, S., Wischnewski, K., Wille, C., and Hubberten, H.-W.: Baseline characteristics of climate, permafrost and land cover from a new permafrost observatory

in the Lena River Delta, Siberia (1998–2011), Biogeosciences, 10, 2105–2128, https://doi.org/10.5194/bg-10-2105-2013, 2013.

Callaghan, T. V., Bergholm, F., Christensen, T. R., Jonasson, C., Kokfelt, U., and Johansson, M.: A new climate era in the sub-Arctic: Accelerating climate changes and multiple impacts, Geophysical Research Letters, 37, https://doi.org/10.1029/2009GL042064, 2010.

Chasar, L. S., Chanton, J. P., Glaser, P. H., Siegel, D. I., and Rivers, J. S.: Radiocarbon and stable carbon isotopic evidence for transport and transformation of dissolved organic carbon, dissolved inorganic carbon, and CH4 in a northern Minnesota peatland, Global Biogeochemical Cycles, 14, 1095–1108, https://doi.org/10.1029/1999GB001221, 2000.

Conrad, R.: Control of microbial methane production in wetland rice fields, Nutrient Cycling in Agroecosystems, 64, 59–69, https://doi.org/10.1023/A:1021178713988, 2002.

Davidson, E. A. and Janssens, I. A.: Temperature sensitivity of soil carbon decomposition and feedbacks to climate change, Nature, 440, 165–173, https://doi.org/10.1038/nature04514, 2006.

Dean, J. F., Middelburg, J. J., Röckmann, T., Aerts, R., Blauw, L. G., Egger, M., Jetten, M. S. M., de Jong, A. E. E., Meisel, O. H., Rasigraf, O., Slomp, C. P., in't Zandt, M. H., and Dolman, A. J.: Methane Feedbacks to the Global Climate System in a Warmer World, Rev. Geophys., 56, 207–250, https://doi.org/10.1002/2017RG000559, 2018.

Deng, J., Gu, Y., Zhang, J., Xue, K., Qin, Y., Yuan, M., Yin, H., He, Z., Wu, L., Schuur, E. A. G., Tiedje, J. M., and Zhou, J.: Shifts of tundra bacterial and archaeal communities along a permafrost thaw gradient in Alaska, Molecular Ecology, 24, 222–234, https://doi.org/10.1111/mec.13015, 2015.

Douglas, T. A., Turetsky, M. R., and Koven, C. D.: Increased rainfall stimulates permafrost thaw across a variety of Interior Alaskan boreal ecosystems, npj Clim Atmos Sci, 3, 1–7, https://doi.org/10.1038/s41612-020-0130-4, 2020.

Elder, C. D., Thompson, D. R., Thorpe, A. K., Hanke, P., Walter Anthony, K. M., and Miller, C. E.: Airborne Mapping Reveals Emergent Power Law of Arctic Methane Emissions, Geophysical Research Letters, 47, e2019GL085707, https://doi.org/10.1029/2019GL085707, 2020.

Elderfield, H. and Schlesinger, W.: Biogeochemistry. An Analysis of Global Change, Earth System Science and Global Change., Geological Magazine, 135, 819–842, https://doi.org/10.1017/S0016756898231505, 1998.

Ernakovich, J. G., Barbato, R. A., Rich, V. I., Schädel, C., Hewitt, R. E., Doherty, S. J., Whalen, E. D., Abbott, B. W., Barta, J., Biasi, C., Chabot, C. L., Hultman, J., Knoblauch, C., Vetter, M. C. Y. L., Leewis, M.-C., Liebner, S., Mackelprang, R., Onstott, T. C., Richter, A., Schütte, U. M. E., Siljanen, H. M. P., Taş, N., Timling, I., Vishnivetskaya, T. A., Waldrop, M. P., and Winkel, M.: Microbiome assembly in thawing permafrost and its feedbacks to climate, Global Change Biology, 28, 5007–5026, https://doi.org/10.1111/gcb.16231, 2022.

Eskelinen, A., Stark, S., and Männistö, M.: Links between plant community composition, soil organic matter quality and microbial communities in contrasting tundra habitats, Oecologia, 161, 113–123, https://doi.org/10.1007/s00442-009-1362-5, 2009.

Faucherre, S., Jørgensen, C. J., Blok, D., Weiss, N., Siewert, M. B., Bang-Andreasen, T., Hugelius, G., Kuhry, P., and Elberling, B.: Short and Long-Term Controls on Active Layer and Permafrost Carbon Turnover Across the Arctic, Journal of Geophysical Research: Biogeosciences, 123, 372–390, https://doi.org/10.1002/2017JG004069, 2018.

Fewster, R. E., Morris, P. J., Ivanovic, R. F., Swindles, G. T., Peregon, A. M., and Smith, C. J.: Imminent loss of climate space for permafrost peatlands in Europe and Western Siberia, Nat. Clim. Chang., 12, 373–379, https://doi.org/10.1038/s41558-022-01296-7, 2022.

Fuchs, M.: Soil organic carbon and nitrogen pools in thermokarst-affected permafrost terrain, phd, Universität Potsdam, 2019.

Ganzert, L., Jurgens, G., Münster, U., and Wagner, D.: Methanogenic communities in permafrost-affected soils of the Laptev Sea coast, Siberian Arctic, characterized by 16S rRNA gene fingerprints, FEMS Microbiology Ecology, 59, 476–488, https://doi.org/10.1111/j.1574-6941.2006.00205.x, 2007.

Grigoriev, M. N.: Cryomorphogenesis in the Lena Delta. Yakutsk, Permafrost Institute Press, 176 pp, 1993.

Hales, B. A., Edwards, C., Ritchie, D. A., Hall, G., Pickup, R. W., and Saunders, J. R.: Isolation and identification of methanogen-specific DNA from blanket bog peat by PCR amplification and sequence analysis, Applied and Environmental Microbiology, https://doi.org/10.1128/aem.62.2.668-675.1996, 1996.

Herbst, T.: Carbon Stocks and Potential Greenhouse Gas Release of Permafrost-affected Active Floodplains in the Lena River Delta, master, Faculty of Environment and Natural Resources, 73 pp., 2022.

560 Hinzman, L. D., Bettez, N. D., Bolton, W. R., Chapin, F. S., Dyurgerov, M. B., Fastie, C. L., Griffith, B., Hollister, R. D., Hope, A., Huntington, H. P., Jensen, A. M., Jia, G. J., Jorgenson, T., Kane, D. L., Klein, D. R., Kofinas, G., Lynch, A. H., Lloyd, A. H., McGuire, A. D., Nelson, F. E., Oechel, W. C., Osterkamp, T. E., Racine, C. H., Romanovsky, V. E., Stone, R. S., Stow, D. A., Sturm, M., Tweedie, C. E., Vourlitis, G. L., Walker, M. D., Walker, D. A., Webber, P. J., Welker, J. M., Winker, K. S., and Yoshikawa, K.: Evidence and Implications of Recent Climate Change in Northern Alaska and Other Arctic 565 Regions, Climatic Change, 72, 251–298, https://doi.org/10.1007/s10584-005-5352-2, 2005.

Holm, S., Walz, J., Horn, F., Yang, S., Grigoriev, M. N., Wagner, D., Knoblauch, C., and Liebner, S.: Methanogenic response to long-term permafrost thaw is determined by paleoenvironment, FEMS Microbiology Ecology, 96, https://doi.org/10.1093/femsec/fiaa021, 2020.

Hugelius, G., Strauss, J., Zubrzycki, S., Harden, J. W., Schuur, E. a. G., Ping, C.-L., Schirrmeister, L., Grosse, G., Michaelson, 570 G. J., Koven, C. D., O'Donnell, J. A., Elberling, B., Mishra, U., Camill, P., Yu, Z., Palmtag, J., and Kuhry, P.: Estimated stocks of circumpolar permafrost carbon with quantified uncertainty ranges and identified data gaps, Biogeosciences, 11, 6573–6593, https://doi.org/10.5194/bg-11-6573-2014, 2014a.

Hugelius, G., Strauss, J., Zubrzycki, S., Harden, J. W., Schuur, E. a. G., Ping, C.-L., Schirrmeister, L., Grosse, G., Michaelson, G. J., Koven, C. D., O'Donnell, J. A., Elberling, B., Mishra, U., Camill, P., Yu, Z., Palmtag, J., and Kuhry, P.: Estimated stocks 575 of circumpolar permafrost carbon with quantified uncertainty ranges and identified data gaps, Biogeosciences, 11, 6573–6593, https://doi.org/10.5194/bg-11-6573-2014, 2014b.

Huissteden, J. van, Maximov, T. C., and Dolman, A. J.: High methane flux from an arctic floodplain (Indigirka lowlands, eastern Siberia): methane flux arctic floodplain Siberia, J. Geophys. Res., 110, n/a-n/a, https://doi.org/10.1029/2005JG000010, 2005.

580 IPCC: IPCC, 2021: Climate Change 2021: The Physical Science Basis. Contribution of Working Group I to the Sixth Assessment Report of the Intergovernmental Panel on Climate Change, Cambridge University Press. In Press., 2021.

Jaatinen, K., Fritze, H., Laine, J., and Laiho, R.: Effects of short- and long-term water-level drawdown on the populations and activity of aerobic decomposers in a boreal peatland, Global Change Biology, 13, 491–510, https://doi.org/10.1111/j.1365-2486.2006.01312.x, 2007.

585 Jongejans, L. L., Liebner, S., Knoblauch, C., Mangelsdorf, K., Ulrich, M., Grosse, G., Tanski, G., Fedorov, A. N., Konstantinov, P. Ya., Windirsch, T., Wiedmann, J., and Strauss, J.: Greenhouse gas production and lipid biomarker distribution in Yedoma and Alas thermokarst lake sediments in Eastern Siberia, Global Change Biology, 27, 2822–2839, https://doi.org/10.1111/gcb.15566, 2021.

Juncher Jørgensen, C., Lund Johansen, K. M., Westergaard-Nielsen, A., and Elberling, B.: Net regional methane sink in High 590 Arctic soils of northeast Greenland, Nature Geosci, 8, 20–23, https://doi.org/10.1038/ngeo2305, 2015.

Keller, J. K. and Bridgham, S. D.: Pathways of anaerobic carbon cycling across an ombrotrophic-minerotrophic peatland gradient, Limnology and Oceanography, 52, 96–107, https://doi.org/10.4319/lo.2007.52.1.0096, 2007.

Knoblauch, C., Beer, C., Sosnin, A., Wagner, D., and Pfeiffer, E.-M.: Predicting long-term carbon mineralization and trace gas production from thawing permafrost of Northeast Siberia, Global Change Biology, 19, 1160–1172, 595 https://doi.org/10.1111/gcb.12116, 2013.

Knoblauch, C., Beer, C., Liebner, S., Grigoriev, M. N., and Pfeiffer, E.-M.: Methane production as key to the greenhouse gas budget of thawing permafrost, Nature Climate Change, 8, 309–312, https://doi.org/10.1038/s41558-018-0095-z, 2018.

Koven, C. D., Ringeval, B., Friedlingstein, P., Ciais, P., Cadule, P., Khvorostyanov, D., Krinner, G., and Tarnocai, C.: Permafrost carbon-climate feedbacks accelerate global warming, PNAS, 108, 14769–14774, 600 https://doi.org/10.1073/pnas.1103910108, 2011.

Kuhn, M. A., Thompson, L. M., Winder, J. C., Braga, L. P. P., Tanentzap, A. J., Bastviken, D., and Olefeldt, D.: Opposing Effects of Climate and Permafrost Thaw on CH4 and CO2 Emissions From Northern Lakes, AGU Advances, 2, e2021AV000515, https://doi.org/10.1029/2021AV000515, 2021.

Kuhry, P., Bárta, J., Blok, D., Elberling, B., Faucherre, S., Hugelius, G., Jørgensen, C. J., Richter, A., Šantrůčková, H., and 605 Weiss, N.: Lability classification of soil organic matter in the northern permafrost region, Biogeosciences, 17, 361–379, https://doi.org/10.5194/bg-17-361-2020, 2020.

Lara, M. J., Lin, D. H., Andresen, C., Lougheed, V. L., and Tweedie, C. E.: Nutrient Release From Permafrost Thaw Enhances CH4 Emissions From Arctic Tundra Wetlands, Journal of Geophysical Research: Biogeosciences, 124, 1560–1573, https://doi.org/10.1029/2018JG004641, 2019.

610 Lee, H., Schuur, E. A. G., Inglett, K. S., Lavoie, M., and Chanton, J. P.: The rate of permafrost carbon release under aerobic and anaerobic conditions and its potential effects on climate, Global Change Biology, 18, 515–527, https://doi.org/10.1111/j.1365-2486.2011.02519.x, 2012.

Li, F., Tianze, S., and Yahai, L.: Snapshot of methanogen sensitivity to temperature in Zoige wetland from Tibetan plateau, Frontiers in Microbiology, https://doi.org/10.3389/fmicb.2015.00131, 2015.

615 Liebner, S., Ganzert, L., Kiss, A., Yang, S., Wagner, D., and Svenning, M. M.: Shifts in methanogenic community composition and methane fluxes along the degradation of discontinuous permafrost, Frontiers in Microbiology, 6, 2015.

Liljedahl, A. K., Boike, J., Daanen, R. P., Fedorov, A. N., Frost, G. V., Grosse, G., Hinzman, L. D., Iijma, Y., Jorgenson, J. C., Matveyeva, N., Necsoiu, M., Raynolds, M. K., Romanovsky, V. E., Schulla, J., Tape, K. D., Walker, D. A., Wilson, C. J., Yabuki, H., and Zona, D.: Pan-Arctic ice-wedge degradation in warming permafrost and its influence on tundra hydrology, 620 Nature Geosci, 9, 312–318, https://doi.org/10.1038/ngeo2674, 2016.

Mann, P. J., Sobczak, W. V., LaRue, M. M., Bulygina, E., Davydova, A., Vonk, J. E., Schade, J., Davydov, S., Zimov, N., Holmes, R. M., and Spencer, R. G. M.: Evidence for key enzymatic controls on metabolism of Arctic river organic matter, Global Change Biology, 20, 1089–1100, https://doi.org/10.1111/gcb.12416, 2014.

McCalley, C. K., Woodcroft, B. J., Hodgkins, S. B., Wehr, R. A., Kim, E.-H., Mondav, R., Crill, P. M., Chanton, J. P., Rich, 625 V. I., Tyson, G. W., and Saleska, S. R.: Methane dynamics regulated by microbial community response to permafrost thaw, Nature, 514, 478–481, https://doi.org/10.1038/nature13798, 2014.

Megonigal, J. P. and Schlesinger, W. H.: Methane-limited methanotrophy in tidal freshwater swamps, Global Biogeochemical Cycles, 16, 35-1-35–10, https://doi.org/10.1029/2001GB001594, 2002.

Meijboom, F. and Noordwijk, M. van: Rhizon soil solu-tion samplers as artificial roots, in: Root ecology and its practical 630 application, Verein für Wurzelforschung, A-9020 Klagenfurt Austria, 793–795, 1991.

Morgenstern, A., Overduin, P. P., Günther, F., Stettner, S., Ramage, J., Schirrmeister, L., Grigoriev, M. N., and Grosse, G.: Thermo-erosional valleys in Siberian ice-rich permafrost, Permafrost and Periglacial Processes, 32, 59–75, https://doi.org/10.1002/ppp.2087, 2021.

Myers-Smith, I. H., Forbes, B. C., Wilmking, M., Hallinger, M., Lantz, T., Blok, D., Tape, K. D., Macias-Fauria, M., Sass-635 Klaassen, U., Lévesque, E., Boudreau, S., Ropars, P., Hermanutz, L., Trant, A., Collier, L. S., Weijers, S., Rozema, J., Rayback, S. A., Schmidt, N. M., Schaepman-Strub, G., Wipf, S., Rixen, C., Ménard, C. B., Venn, S., Goetz, S., Andreu-Hayles, L., Elmendorf, S., Ravolainen, V., Welker, J., Grogan, P., Epstein, H. E., and Hik, D. S.: Shrub expansion in tundra ecosystems: dynamics, impacts and research priorities, Environ. Res. Lett., 6, 045509, https://doi.org/10.1088/1748-9326/6/4/045509, 2011.

640 Oblogov, G. E., Vasiliev, A. A., Streletskaya, I. D., Zadorozhnaya, N. A., Kuznetsova, A. O., Kanevskiy, M. Z., and Semenov, P. B.: Methane Content and Emission in the Permafrost Landscapes of Western Yamal, Russian Arctic, Geosciences, 10, 412, https://doi.org/10.3390/geosciences10100412, 2020.

Obu, J., Westermann, S., Bartsch, A., Berdnikov, N., Christiansen, H. H., Dashtseren, A., Delaloye, R., Elberling, B., Etzelmüller, B., Kholodov, A., Khomutov, A., Kääb, A., Leibman, M. O., Lewkowicz, A. G., Panda, S. K., Romanovsky, V., 645 Way, R. G., Westergaard-Nielsen, A., Wu, T., Yamkhin, J., and Zou, D.: Northern Hemisphere permafrost map based on TTOP modelling for 2000–2016 at 1 km2 scale, Earth-Science Reviews, 193, 299–316, https://doi.org/10.1016/j.earscirev.2019.04.023, 2019.

Olefeldt, D., Turetsky, M. R., Crill, P. M., and McGuire, A. D.: Environmental and physical controls on northern terrestrial methane emissions across permafrost zones, Global Change Biology, 19, 589–603, https://doi.org/10.1111/gcb.12071, 2013.

650 Osterkamp, T. E., Jorgenson, M. T., Schuur, E. a. G., Shur, Y. L., Kanevskiy, M. Z., Vogel, J. G., and Tumskoy, V. E.: Physical and ecological changes associated with warming permafrost and thermokarst in Interior Alaska, Permafrost and Periglacial Processes, 20, 235–256, https://doi.org/10.1002/ppp.656, 2009.

Paul, S., Küsel, K., and Alewell, C.: Reduction processes in forest wetlands: Tracking down heterogeneity of source/sink functions with a combination of methods, Soil Biology and Biochemistry, 38, 1028–1039, 655 https://doi.org/10.1016/j.soilbio.2005.09.001, 2006.

Pegoraro, E., Mauritz, M., Bracho, R., Ebert, C., Dijkstra, P., Hungate, B. A., Konstantinidis, K. T., Luo, Y., Schädel, C., Tiedje, J. M., Zhou, J., and Schuur, E. A. G.: Glucose addition increases the magnitude and decreases the age of soil respired carbon in a long-term permafrost incubation study, Soil Biology and Biochemistry, 129, 201–211, https://doi.org/10.1016/j.soilbio.2018.10.009, 2019.

660 R Core Team: R: A Language and Environment for Statistical Computing, R Foundation for Statistical Computing, Vienna, Austria, 2021.

Rantanen, M., Karpechko, A. Y., Lipponen, A., Nordling, K., Hyvärinen, O., Ruosteenoja, K., Vihma, T., and Laaksonen, A.: The Arctic has warmed nearly four times faster than the globe since 1979, Commun Earth Environ, 3, 1–10, https://doi.org/10.1038/s43247-022-00498-3, 2022.

665 Robertson, G. P., Coleman, D. C., Sollins, P., and Bledsoe, C. S.: Standard Soil Methods for Long-term Ecological Research, Oxford University Press, 481 pp., 1999.

Rößger, N., Sachs, T., Wille, C., Boike, J., and Kutzbach, L.: Seasonal increase of methane emissions linked to warming in Siberian tundra, Nat. Clim. Chang., 12, 1031–1036, https://doi.org/10.1038/s41558-022-01512-4, 2022.

Schädel, C., Schuur, E. A. G., Bracho, R., Elberling, B., Knoblauch, C., Lee, H., Luo, Y., Shaver, G. R., and Turetsky, M. R.:
670 Circumpolar assessment of permafrost C quality and its vulnerability over time using long-term incubation data, Glob Change Biol, 20, 641–652, https://doi.org/10.1111/gcb.12417, 2014.

Schädel, C., Beem-Miller, J., Aziz Rad, M., Crow, S. E., Hicks Pries, C. E., Ernakovich, J., Hoyt, A. M., Plante, A., Stoner, S., Treat, C. C., and Sierra, C. A.: Decomposability of soil organic matter over time: the Soil Incubation Database (SIDb, version 1.0) and guidance for incubation procedures, Earth System Science Data, 12, 1511–1524, https://doi.org/10.5194/essd-
675 12-1511-2020, 2020.

Schirrmeister, L., Kunitsky, V., Grosse, G., Wetterich, S., Meyer, H., Schwamborn, G., Babiy, O., Derevyagin, A., and Siegert, C.: Sedimentary characteristics and origin of the Late Pleistocene Ice Complex on north-east Siberian Arctic coastal lowlands and islands – A review, Quaternary International, 241, 3–25, https://doi.org/10.1016/j.quaint.2010.04.004, 2011.

Schirrmeister, L., Froese, D., Tumskoy, V., Grosse, G., and Wetterich, S.: PERMAFROST AND PERIGLACIAL FEATURES
680 | Yedoma: Late Pleistocene Ice-Rich Syngenetic Permafrost of Beringia, in: Encyclopedia of Quaternary Science, Elsevier, 542–552, https://doi.org/10.1016/B978-0-444-53643-3.00106-0, 2013.

Schneider, J., Grosse, G., and Wagner, D.: Land cover classification of tundra environments in the Arctic Lena Delta based on Landsat 7 ETM+ data and its application for upscaling of methane emissions, Remote Sensing of Environment, 113, 380–391, https://doi.org/10.1016/j.rse.2008.10.013, 2009.

685 Schuur, E. a. G., McGuire, A. D., Schädel, C., Grosse, G., Harden, J. W., Hayes, D. J., Hugelius, G., Koven, C. D., Kuhry, P., Lawrence, D. M., Natali, S. M., Olefeldt, D., Romanovsky, V. E., Schaefer, K., Turetsky, M. R., Treat, C. C., and Vonk, J. E.: Climate change and the permafrost carbon feedback, Nature, 520, 171–179, https://doi.org/10.1038/nature14338, 2015.

Schwamborn, G., Rachold, V., and Grigoriev, M. N.: Late Quaternary sedimentation history of the Lena Delta, Quaternary International, 89, 119–134, https://doi.org/10.1016/S1040-6182(01)00084-2, 2002.

690 Serreze, M. C., Walsh, J. E., Chapin, F. S., Osterkamp, T., Dyurgerov, M., Romanovsky, V., Oechel, W. C., Morison, J., Zhang, T., and Barry, R. G.: Observational Evidence of Recent Change in the Northern High-Latitude Environment, Climatic Change, 46, 159–207, https://doi.org/10.1023/A:1005504031923, 2000.

Siewert, M. B., Hugelius, G., Heim, B., and Faucherre, S.: Landscape controls and vertical variability of soil organic carbon storage in permafrost-affected soils of the Lena River Delta, CATENA, 147, 725–741,
695 https://doi.org/10.1016/j.catena.2016.07.048, 2016.

Soil Survey Staff: Keys to Soil Taxonomy, 12th ed., Twelfth Edition, USDA-Natural Resources Conservation Service, Washington, DC, 360 pp., 2014.

Spencer, R. G. M., Mann, P. J., Dittmar, T., Eglinton, T. I., McIntyre, C., Holmes, R. M., Zimov, N., and Stubbins, A.: Detecting the signature of permafrost thaw in Arctic rivers, Geophysical Research Letters, 42, 2830–2835,
700 https://doi.org/10.1002/2015GL063498, 2015.

Strauss, J., Schirrmeister, L., Grosse, G., Wetterich, S., Ulrich, M., Herzschuh, U., and Hubberten, H.-W.: The deep permafrost carbon pool of the Yedoma region in Siberia and Alaska, Geophysical Research Letters, 40, 6165–6170, https://doi.org/10.1002/2013GL058088, 2013a.

Strauss, J., Schirrmeister, L., Grosse, G., Wetterich, S., Ulrich, M., Herzschuh, U., and Hubberten, H.-W.: The deep permafrost carbon pool of the Yedoma region in Siberia and Alaska, Geophysical Research Letters, 40, 6165–6170, https://doi.org/10.1002/2013GL058088, 2013b.

Symons, G. E. and Buswell, A. M.: The methane fermentation of carbohydrates., vol. 55, J. Am. Chem. Soc., 2028–2036, 1993.

Tabari, H.: Climate change impact on flood and extreme precipitation increases with water availability, Sci Rep, 10, 13768, https://doi.org/10.1038/s41598-020-70816-2, 2020.

Thauer, R. K.: Biochemistry of methanogenesis: a tribute to Marjory Stephenson:1998 Marjory Stephenson Prize Lecture, Microbiology, 144, 2377–2406, https://doi.org/10.1099/00221287-144-9-2377, 1998.

Theisen, A. R. and Murrell, J. C.: Facultative Methanotrophs Revisited, Journal of Bacteriology, 187, 4303–4305, https://doi.org/10.1128/JB.187.13.4303-4305.2005, 2005.

Treat, C. C., Natali, S. M., Ernakovich, J., Iversen, C. M., Lupascu, M., McGuire, A. D., Norby, R. J., Roy Chowdhury, T., Richter, A., Šantrůčková, H., Schädel, C., Schuur, E. A. G., Sloan, V. L., Turetsky, M. R., and Waldrop, M. P.: A pan-Arctic synthesis of CH_4 and CO_2 production from anoxic soil incubations, Glob Change Biol, 21, 2787–2803, https://doi.org/10.1111/gcb.12875, 2015.

Treat, C. C., Marushchak, M. E., Voigt, C., Zhang, Y., Tan, Z., Zhuang, Q., Virtanen, T. A., Räsänen, A., Biasi, C., Hugelius, G., Kaverin, D., Miller, P. A., Stendel, M., Romanovsky, V., Rivkin, F., Martikainen, P. J., and Shurpali, N. J.: Tundra landscape heterogeneity, not interannual variability, controls the decadal regional carbon balance in the Western Russian Arctic, Global Change Biology, 24, 5188–5204, https://doi.org/10.1111/gcb.14421, 2018.

Turetsky, M. R., Abbott, B. W., Jones, M. C., Walter Anthony, K., Olefeldt, D., Schuur, E. A. G., Koven, C., McGuire, A. D., Grosse, G., Kuhry, P., Hugelius, G., Lawrence, D. M., Gibson, C., and Sannel, A. B. K.: Permafrost collapse is accelerating carbon release, Nature, 569, 32–34, https://doi.org/10.1038/d41586-019-01313-4, 2019.

Wagner, D., Gattinger, A., Embacher, A., Pfeiffer, E.-M., Schloter, M., and Lipski, A.: Methanogenic activity and biomass in Holocene permafrost deposits of the Lena Delta, Siberian Arctic and its implication for the global methane budget, Global Change Biology, 13, 1089–1099, https://doi.org/10.1111/j.1365-2486.2007.01331.x, 2007.

Waldrop, M. P., Wickland, K. P., White Iii, R., Berhe, A. A., Harden, J. W., and Romanovsky, V. E.: Molecular investigations into a globally important carbon pool: permafrost-protected carbon in Alaskan soils, Global Change Biology, 16, 2543–2554, https://doi.org/10.1111/j.1365-2486.2009.02141.x, 2010.

Walz, J., Knoblauch, C., Böhme, L., and Pfeiffer, E.-M.: Regulation of soil organic matter decomposition in permafrost-affected Siberian tundra soils - Impact of oxygen availability, freezing and thawing, temperature, and labile organic matter, Soil Biology and Biochemistry, 110, 34–43, https://doi.org/10.1016/j.soilbio.2017.03.001, 2017.

Walz, J., Knoblauch, C., Tigges, R., Opel, T., Schirrmeister, L., and Pfeiffer, E.-M.: Greenhouse gas production in degrading ice-rich permafrost deposits in northeastern Siberia, Biogeosciences, 15, 5423–5436, https://doi.org/10.5194/bg-15-5423-2018, 2018.

Wang, P., Huang, Q., Tang, Q., Chen, X., Yu, J., Pozdniakov, S. P., and Wang, T.: Increasing annual and extreme precipitation in permafrost-dominated Siberia during 1959–2018, Journal of Hydrology, 603, 126865, https://doi.org/10.1016/j.jhydrol.2021.126865, 2021.

Washburn, A. L.: Periglacial processes and environment., St. Martin's Press, New York, 1973.

Westermann, P.: Temperature regulation of methanogenesis in wetlands, Chemosphere, 26, 321–328, https://doi.org/10.1016/0045-6535(93)90428-8, 1993.

Yavitt, J. B., Williams, C. J., and Wieder, R. K.: Production of methane and carbon dioxide in peatland ecosystems across North America: Effects of temperature, aeration, and organic chemistry of peat, Geomicrobiology Journal, 14, 299–316, https://doi.org/10.1080/01490459709378054, 1997.

Yavitt, J. B., Basiliko, N., Turetsky, M. R., and Hay, A. G.: Methanogenesis and Methanogen Diversity in Three Peatland Types of the Discontinuous Permafrost Zone, Boreal Western Continental Canada, Geomicrobiology Journal, 23, 641–651, https://doi.org/10.1080/01490450600964482, 2006.

750 Zhu, X., Wu, T., Li, R., Xie, C., Hu, G., Qin, Y., Wang, W., Hao, J., Yang, S., Ni, J., and Yang, C.: Impacts of Summer Extreme Precipitation Events on the Hydrothermal Dynamics of the Active Layer in the Tanggula Permafrost Region on the Qinghai-Tibetan Plateau, Journal of Geophysical Research: Atmospheres, 122, 11,549-11,567, https://doi.org/10.1002/2017JD026736, 2017.

755